Z. Kristallogr. **225** (2010) 94–102 / **DOI** 10.1524/zkri.2010.1202
© by Oldenbourg Wissenschaftsverlag, München

Collecting 3D electron diffraction data by the rotation method

Daliang Zhang[I, II], Peter Oleynikov[I], Sven Hovmöller[*, I] and Xiaodong Zou[I]

[I] Inorganic and Structural Chemistry, Department of Materials and Environmental Chemistry, Stockholm University, 106 91 Stockholm, Sweden
[II] State Key Laboratory of Inorganic Synthesis and Preparative Chemistry, Jilin University, Changchun, 130012, China

Received June 30, 2009; accepted November 13, 2009

Electron diffraction / Data collection / 3D diffraction data

Abstract. A new method for collecting complete three-dimensional electron diffraction data is described. Diffraction data is collected by combining electron beam tilt at many very small steps, with rotation of the crystal in a few but large steps. A number of practical considerations are discussed, as well as advantages and disadvantages compared to other methods of collecting electron diffraction data.

1. Introduction

Electron diffraction offers some very attractive advantages compared to X-ray diffraction. The most important is that extremely small crystals can be used. For electrons, a crystal size of 10 nm in all three dimensions is sufficient; several million times smaller than the smallest single crystal (about 10 μm^3) that is currently needed for collecting single crystal X-ray diffraction data on a synchrotron (Moukhametzianov *et al.*, 2008). Unfortunately, there are also disadvantages with electrons, the main ones being multiple diffraction and the lack of automated systems for collecting 3D diffraction data. The method presented here is aimed at remedying these shortcomings.

The wavelength of electrons is very short; about 0.02–0.03 Å when an accelerating voltage of 200–400 kV (kilovolt) is used. This is some 50 times shorter than what is commonly used for X-ray diffraction, ~1.0–1.5 Å. As a consequence, the Ewald sphere has a radius 50 times larger for electrons, making its surface almost flat. A single still photo of a crystal taken by electron diffraction will show complete diffraction spots out to or even beyond 1.0 Å resolution, if the crystal quality is sufficient. The diffraction pattern will be an undistorted flat section through reciprocal space. If the crystal is aligned, for example with the incident electron beam along the *c* axis, a complete *hk*0 diffraction pattern can be recorded in a single frame. A typical exposure time is just seconds.

Electrons interact much stronger with matter than X-rays do, making it possible to study extremely small crystals. This strong interaction makes multiple diffraction a serious problem, even for crystals only a few nanometres thick. Because the Ewald sphere is almost flat, many reflections are simultaneously in diffracting conditions. This is especially true for diffraction patterns taken near zone axis directions or major diagonals, such as ⟨100⟩, ⟨110⟩, ⟨111⟩ and so on.

The presence of multiple diffraction can often be seen directly in a diffraction pattern in two ways. Systematically absent reflections (forbidden by symmetry) are present and the intensity variation of reflections in the diffraction pattern is small. For very thin (a few nm) crystals the diffraction pattern is dominated by single scattering events and is thus closer to the kinematical pattern, as in X-ray diffraction. Diffraction patterns from thick crystals are usually dominated by dynamical scattering, which may make the data unsuitable for solving or refining the crystal structure. The systematically absent reflections may have considerable intensities for thick crystals, but can also be very weak, especially if the crystal is perfectly aligned and flat. Thus, clear systematic absences cannot be used as a criterion for kinematic data.

It was long thought that electron diffraction data could not be used for solving crystal structures, as is done with X-ray diffraction, because of the strong dynamical effects (Cowley, 1992). For weakly scattering crystals, such as proteins (Unwin, Henderson, 1975) and organic molecules (Dorset, 1995) the situation was better. Yet, successful examples of structural analysis by electron diffraction were presented already in the1950s (Vainshtein, 1964). The specialized technique of electron texture patterns developed in Moscow could also be used to collect quasi-kinematical data on clay minerals (Zvyagin *et al.*, 2003). It was only after 1990 that serious attempts were made to collect and quantify electron diffraction patterns from inorganic crystals. A computer program for fast and accurate estimation of intensities in electron diffraction patterns was then developed; ELD (Zou *et al.*, 1993). In spite of the general pessimism, if great care is taken to collect the diffraction data only from the very thinnest part of the crystal, quasi-kinematical data can be obtained also from crystals containing heavy elements, such as $Ti_{11}Se_4$ (Weirich *et al.*, 1996), Zr_2Se (Weirich *et al.*, 2000) and the very complex ν-AlFeCr with some 130 atoms in the unit cell (Zou *et al.*, 2003).

Although not impossible, it remained a very hard work, demanding great skill and patience from the operator, to collect useful electron diffraction patterns with the stan-

* Correspondence author (e-mail: sven.hovmoller@mmk.su.se)

dard method, called selected-area electron diffraction (SAED). The invention of the electron precession method, by Roger Vincent and Paul Midgley in Bristol (1994) brought new hope to the field of quantitative electron diffraction. By rotating (at the speed of several Hertz) the electron beam in a conical way around the optical axis, a diffraction pattern is obtained that is the sum of a continuous set of misaligned diffraction patterns. The precession angle is typically $\sim 1°-3°$, and this is enough to make sure only a few reflections are in Bragg condition at any one moment, thus making dynamical effects much less pronounced than with the SAED technique.

A few groups developed their own precession units, notably in Chicago (Own *et al.*, 2004), Oslo (Gjønnes *et al.*, 1998) and Milano (Gemmi *et al.*, 2001). However, it was only after the launching of a commercial product, the Spinning Star (NanoMEGAS 2004), that the precession method really took off.

With electron precession, it becomes much easier to collect high-quality electron diffraction patterns. While SAED patterns must be taken from crystals aligned to better than 0.1° from the perfect zone axis, a precession electron diffraction (PED) pattern will look very symmetrical (*i.e.* well-aligned) even if it is tilted by up to $\sim 1°$. In most cases, the PED patterns also go to higher resolution than an SAED pattern collected from the same crystal. While an SAED pattern is a nearly flat, very thin section through reciprocal space, PED generates integrated intensities.

Many inorganic compounds have a short ($\sim$4 Å) unit cell dimension. When viewed along this direction, most of the atoms, especially metals, can be resolved. Then it is possible to solve the structure from a single high-resolution transmission electron microscopy (HRTEM) image or a single diffraction pattern (SAED or PED). Metal oxides of Nb, W or Ta and chalcogenides, such as $Ti_{11}Se_4$, $ZrSe_2$ etc. often form such crystals. However, when the shortest unit cell dimension is larger (>5 Å), it becomes necessary to collect data from several projections, *i.e.* along [100], [010] and [001]. Recently, several zeolites with unit cell dimensions in the range 14–57 Å have been solved by combining electron crystallography and powder X-ray diffraction (Gramm *et al.*, 2006, Baerlocher *et al.* 2007). These are the most complicated zeolites ever solved by crystallography (including X-ray crystallography). Zeolites are examples of compounds that are often better suited for structure determination by electrons than by X-rays, mainly because they are often very hard to crystallize as single crystals in μm sizes. In many cases when the unit cell dimensions are large (>10 Å), it is necessary to collect HRTEM images and SAED or PED patterns from a large number of projections. The very complex intermetallic compound ν-AlFeCr was solved in this way, from 13 projections – most of them obtained with both HRTEM and SAED data. ν-AlFeCr is hexagonal with unit cell dimension $a = b = 40.7$ Å, $c = 12.5$ Å. Although doable, the structure determination is extremely time-consuming. It became imperative to develop new methods for collecting complete 3-dimensional electron diffraction data.

Recently, an electron diffraction tomography technique has been developed (Kolb *et al.*, 2007), using scanning transmission electron microscopy (STEM) combined with precession electron diffraction. A computer-controlled specimen stage is used and diffraction patterns are taken every 1° by rotating the specimen holder. Very small areas of the crystal are exposed in each frame. During every exposure, the electron beam is precessed in order to collect more reflections and to integrate over the whole reflections.

We wanted to develop a method for collecting complete 3D electron diffraction data in a standard TEM instrument. While precession is excellent for obtaining high-quality diffraction data from a zone axis or major diagonal, it is less well suited for collecting complete 3D diffraction data. The problem is that in each frame there will be many partially recorded reflections. It is very difficult to sort out which reflections that are fully recorded and which are only partially integrated. The same problem was realized in X-ray crystallography in the 1970ies and led Uli Arndt and Alan Wonnacott (1977) to develop the oscillation/rotation method. We now want to develop an analogous way of collecting 3D diffraction data in the transmission electron microscope, *i.e.* a single crystal electron diffractometer, which can collect single crystal diffraction data from nano-sized crystals, million times smaller than the smallest ones that can be studied by X-ray diffraction using synchrotrons.

2. Experimental and methods

2.1 Experimental

The 3D electron diffraction data were obtained in a JEOL JEM2100 TEM operated at 200 kV. A double tilt holder was used for the data collection. This holder is capable of 80° (± 40°) alpha rotations (around the axis of the specimen holder, *i.e.* the goniometer) and 60° (±30°) beta rotations (*i.e.* around an axis which is perpendicular to alpha). Only the alpha rotation was used during our data collection. The beta rotations were used for the zone axis search during the instrument calibration as will be described later. Electron diffraction patterns were recorded by an upper mounted Gatan ES500W Erlangshen camera and a bottom mounted Gatan SC1000 ORIUS CCD camera. The TEM and cameras were controlled by scripts written in Gatan's DigitalMicrograph.

A sample of $K_2O \cdot 7\,Nb_2O_5$ (space group *P4/mbm* (no. 127), $a = b = 27.5$ Å, $c = 3.94$ Å) which is stable under the electron beam was used as a test object. Two unit cell parameters of the crystal are quite large, resulting in a significant number of reflections close to or at exact Bragg condition, when viewed down the shorter *c* axis. The tetragonal symmetry of the crystal is very useful for investigating the quality of the intensities during the data analysis. The structure was suggested from electron crystallography (Li *et al.*, 1992) and the isomorphous compound $Tl_2O \cdot 7\,Nb_2O_5$ has been solved by X-ray crystallography (Bhide, Gasparin, 1979). A small amount of the $K_2O \cdot 7\,Nb_2O_5$ sample was crushed heavily before it was dispersed by ethanol. After ultrasonic treatment, a drop was taken from the ethanol solution and transferred to a copper grid covered by a holey carbon film.

2.2 The rotation method

During the data collection the electron beam is rotated relative to a static crystal by electromagnetic coils. In the case of X-ray diffraction, a large mechanical sample holder is usually used to perform precise rotation. Electromagnetic coils in a TEM can give even more precise rotation than X-ray diffractometers; the rotation steps can be as small as 0.0005° on the JEM 2100 TEM. However, the electron beam can only be rotated in a range of ±3° to ±5° (depending on the TEM; in our case ±5°). To collect 3D electron diffraction data, the rotation method combines rotations of both the electron beam and the goniometer. The data collection can start from any orientation of the crystal, and there is no need to align the crystal. First, a series of electron diffraction patterns is collected within the limit of the beam rotation. The crystal is kept stationary during the data collection. Then the crystal is tilted by a given angle using the goniometer rotation, and another series of electron diffraction patterns is collected. This procedure is repeated until the limit of the goniometer rotation is reached. The rotation method can be used in either selected area electron diffraction (SAED) mode or nano-beam electron diffraction (NBD) mode. The whole data collection can be done automatically; the rotation steps of the electron beam and the goniometer and the exposure time are given by the users.

2.3 Electron beam rotation

The electron beam rotation is done using the beam tilt function on the TEM. The beam tilt of the TEM is introduced by a pair of condenser lens (CL) deflection coils. An upper CL deflection coil tilts the electron beam off the optical axis and moves the electron beam away from the crystal, while a lower CL deflection coil brings the electron beam back onto the crystal, so that the electron beam remains at the same position on the crystal under the electron beam rotation (Fig. 1).

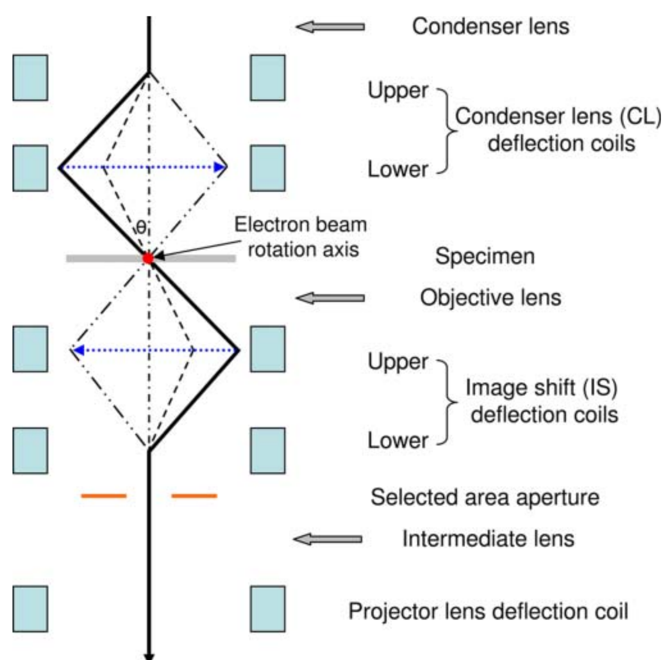

Fig. 1. A ray path diagram of the electron beam rotation. The blue dotted arrow indicates the movement of the electron beam during electron beam rotation. The rotation axis marked as a red dot is perpendicular to the paper in this case.

Although the electron beam can be brought to the same position on the crystal after a beam tilt, it has been brought off the optical axis (see Fig. 1), resulting in a displacement of the direct beam in diffraction mode. Thus we must use extra deflection coils under the specimen to compensate for the displacement so that the direct beam remains at the same position on the diffraction patterns, *i.e.* descan the electron beam. There are two ways of achieving this: by using the image shift (IS) deflection coils and by using the projector lens deflection coils. We choose to use IS deflection coils since they are located above the intermediate lenses, so that the settings of descan will be independent of the choice of camera lengths. If the projector lens deflection coils would be chosen, different settings of descan would have been needed for different camera lengths, since projector lens deflection coils are located below the intermediate lenses (see Fig. 1).

2.3.1 Alignment of electron beam rotation

The IS deflection coils below the specimen should be synchronized with the CL deflection coils above the specimen, so that during the electron beam rotation, the direct beam always remains at the same position on the detector. In addition, the upper and lower IS deflection coils should work simultaneously so that the image does not move during the electron beam rotation. Since the rotation method introduces a large number of sequential beam tilts, it is necessary to make the alignment of the descan for all the beam tilt angles, which can be very time consuming. Since all the deflection coils are computer controlled, the alignment parameters can be stored and reloaded. It is only necessary to do the alignment of the electron beam rotation once per session, after the alignment of the TEM. We found that the lens currents for the IS deflection coils and the CL deflection coils have a very good linear relation within ±2° beam tilt angles for the JEM 2100 TEM (see supplementary Fig. S1), so that the alignment can be done using only one or two different beam tilt angles. The alignment of electron beam rotation can be done automatically by software, using the cross-correlation method.

It should be mentioned that the electron beam in electron rotation has a similar ray path as in electron precession (Avilov *et al.*, 2007), except that the beam is tilted along a line in this rotation technique, whereas it is tilted around in a circle in precession. Unlike in the rotation technique, for electron precession diffraction a fixed beam tilt angle is used and the alignment of descan coils is usually done manually.

As a standard alignment procedure, the electron beam is tilted for a certain angle by the CL deflection coils. As a result, a displacement of the direct beam can be observed in diffraction mode. The direct beam is moved back to the original position by changing the currents of both IS deflection coils. After this, the crystal observed in image mode may have a certain displacement from its pre-

vious position. Then only the upper IS deflection coil is used to move the image of the crystal back in the image mode. These alignments in diffraction and image modes are iterated until both the direct beam in diffraction mode and the image in image mode remain at the same positions. The alignment parameters for this beam tilt angle are saved. The alignment parameters for other angles can be calculated by interpolation. All the alignment can be done automatically by a computer program.

2.3.2 Calibration of the beam tilt angles

The electron beam tilt is generated by the upper CL deflection coil. The exact tilt angles of the electron beam have to be calibrated. This is done by measuring the displacement of the direct beam on the diffraction pattern of a standard powder sample, for example Al-powder or Au-powder.

The relation between the beam tilt angle (θ_T) and the Bragg angle (θ_B) for a diffraction ring is

$$\frac{\sin\theta_T}{\sin\theta_B} = \frac{R_T}{R_B} \tag{1}$$

where R_T is the displacement of the direct beam and R_B is the radius of the diffraction ring. R_T and R_B can be measured directly from the diffraction pattern, and θ_B can be calculated from Bragg's law, knowing the corresponding d-value of the ring and the electron wavelength:

$$\sin\theta_B = \frac{\lambda}{2d} \tag{2}$$

The beam tilt angle θ_T can then be calculated from

$$\sin\theta_T = \frac{\lambda R_T}{2dR_B} \tag{3}$$

Since the tilt angle is usually quite small ($\pm 2°$), the movement in the direct beam is linearly related to the electric current change in the deflection coils. It is enough to calibrate a number of tilt angles and interpolate for other angles.

The deflection coils are equipped with *x*- and *y* deflectors. It is possible to calibrate the tilt angles along both *x*- and *y*-directions. This is done by using only one of the deflectors to tilt the electron beam and make the calibration accordingly. The calibration needs only to be done once and the calibration parameters can be stored.

2.4 The rotation of goniometer

During the collection of a 3D electron diffraction data set, the tilts of the electron beam are alternated with goniometer rotations. Therefore, the rotation axis of the electron beam should be aligned with the rotation axis of the goniometer. In addition, the rotation angles from both rotations should be calibrated. On the other hand, when the specimen is rotated by the goniometer, often the crystal may show a certain displacement upon goniometer rotation even when the eucentric height is already well aligned. It is not sufficient to calibrate the sample stage in order to solve this problem, since the accuracy of the goniometer is not high enough. A crystal tracking procedure should be applied to make sure that the same area of the crystal is used during the complete data collection.

2.4.1 The alignment between the electron beam and the goniometer rotations

It is essential that the electron beam tilt direction coincides with the alpha tilt axis of the goniometer. The orientation of the alpha tilt axis can be calibrated. This is done by using a standard single crystal sample with known unit cell. Diffraction patterns with Laue circles are recorded when the crystal is tilted away from a certain zone axis (preferably with low indices) by the goniometer rotation. Then the rotation axis of the goniometer can be calculated from the position of the Laue circle center (Fig. 2a). Generally, this procedure should only be done once for a goniometer on a TEM. If the CL *x*- and *y*-deflectors are calibrated, the electron beam tilt axis can be accurately tuned, to make it coincide exactly with the goniometer rotation axis.

In addition to the orientation of the rotation axes, the goniometer and the electron beam rotation angles also need to be consistent. Since there might be errors in the

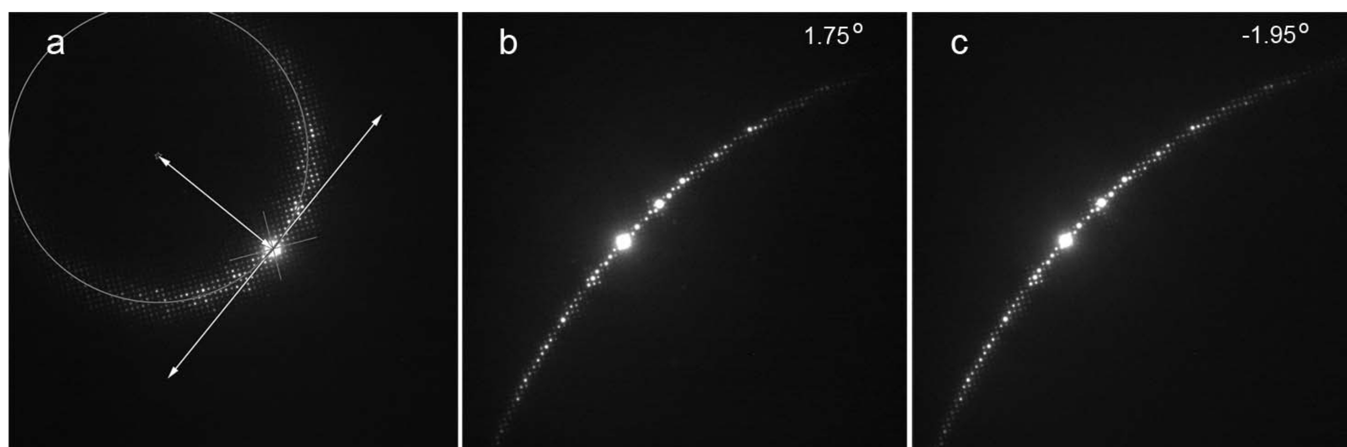

Fig. 2. (**a**) A Laue circle tilted away from a well aligned [001] zone axis, from which the tilt axis of goniometer has been determined as indicated by a white line. (**b**) and (**c**) are the common patterns found from the overlap between two adjacent beam tilt series before and after a 3.5° goniometer rotation. (**b**) 1.75° beam tilt before the goniometer rotation. (**c**) −1.95° beam tilt after the goniometer rotation. Thus, the rotation angle of the specimen given by goniometer rotation is calculated as 3.7°.

goniometer rotation and the electron beam might cause some additional tilt of the crystal, we recommend making the beam tilt coverage slightly larger than the goniometer rotation step, ensuring some overlap between adjacent beam rotation series. For example, the goniometer can be rotated in a step of 3.5° if the range of the electron beam rotation is 4°. It is possible to identify the electron diffraction patterns with the same or similar orientation within the overlapping region of the adjacent beam rotation series, see Figs. 2b and 2c. If the error of the goniometer rotation is smaller than the overlap angle; the data collection will be continuous without gaps. Both the rotation angles of the goniometer and the crystal tilting can be corrected in a data processing procedure using these overlaps.

2.4.2 Crystal tracking procedure

In order to make sure that the same area of the crystal is in the electron beam during the goniometer rotation, a crystal tracking procedure should be applied. Typically, the relative shift of the specimen is calculated by 2D cross-correlation of two images taken before and after the goniometer rotation. Thus, the relative shift of the crystal must be calculated after each goniometer rotation so that the crystal can be shifted back to its original position. The crystal tracking is done by switching the TEM to the diffraction image mode (DIFFMAG). The major reason for using the DIFFMAG mode instead of the standard image mode (MAG) lies in the fact that the settings of the IS deflection coils in DIFFMAG will remain unchanged. After the relative shift has been calculated, the crystal is ready to be moved back to its original position. In the case of bright field TEM tomography, this task is normally done electronically by the TEM image shift function which doesn't move the crystal physically. It can be used in SAED mode, since the IS deflection coils used for the IS function are placed above the imaging plane of the objective lens. This cannot be applied for the NBD mode, because the electron beam will move together with the specimen. On the other hand, the IS deflection coils are involved in electron beam rotation. Therefore, this task is performed by the program controlled stage shift of goniometer, without influencing any coils. Unfortunately, the mechanical goniometer shift can not be controlled with high precision. The actual stage shift should be split into smaller sub-movements. After each sub-movement a new image is acquired in order to calculate the remaining shift. After a few iterations, the crystal position is close enough to the original point. In the case of NBD, the basic crystal tracking procedure is the same as in the SAED mode. An extra operation is required in order to make the electron beam parallel by changing the CL current, since the illumination area is too small for the crystal tracking in the NBD mode. Sometimes, it is necessary to use higher beam brightness by changing the spot size.

2.4.3 Stage shift calibration

The stage shift function implies shifts in both x and y directions. In order to make all stage movements effective during crystal tracking, these shifts must be calibrated a priori, which includes calibration of both x- and y-axes directions and distortion. The calibration is done in the TEM image mode. The maximum of the cross-correlation function tells us the exact direction and the amplitude of the movement during the stage shift.

2.5 Data collection procedure for the rotation method

All the data sets presented in the paper were collected in the SAED mode. The standard data collection experiment workflow using SAED can be described as follows:

a. The TEM machine should be aligned properly following the standard alignment instruction before the experiment starts. The alignment usually includes the illumination system adjustment, CL astigmatism correction, the centering of the current and voltage axes etc. Special care should be taken during the alignment of the CL deflection coils shift and tilt so that the observed electron diffraction pattern remains stationary during electron beam tilt. The eucentric height of the specimen should be adjusted as accurately as possible minimizing sample movements during the goniometer rotation.
b. Make sure that the following calibrations have been made: the beam tilt angles according to 2.3.2, the stage shift according to 2.4.3 and the goniometer rotation axis according to 2.4.1. These calibrations only need to be done once for each TEM.
c. Align CL and IS deflection coils according to 2.3.1.
d. Select a thin area of a crystal using a SAED aperture and adjust the selected crystal to the eucentric height. The crystal is preferably at the centre of the TEM grid.
e. Specify the total rotation range and rotation step as the primary data collection parameters.
f. Record a bright field image as the reference point at the original crystal position.
g. Switch to diffraction mode. Rotate the beam sequentially with the selected beam tilt step. Record electron diffraction patterns after each beam tilt step. In our case a typical rotation series contains 80 frames collected with 0.05° beam tilt steps, covering a range of 4°.
h. Rotate the goniometer by a predetermined fixed angle (3.5° in our case allowing some overlap between the data series) after each rotation series of data collection.
i. Switch to image mode and acquire an image. Calculate the relative movement of the crystal from its original position by 2D cross-correlation.
j. Move the crystal back using the stage shift.
k. Repeat steps g–j until the complete diffraction data set is collected.

3. Results and discussions

Firstly, several series of rotation diffraction data were collected by only the goniometer rotation with different tilt

steps, such as 0.2°, 0.5°, 1°, in the range from −18° to +18°. A movie in the standard MS Windows format was recorded and can be played (see supplementary information).

As for the rotation step, the manufacturer only guarantees 0.1° accuracy of the goniometer, which is also the accuracy we found. When the program requested the goniometer to rotate by ≤0.1° steps, quite often the tilt commands sent to the goniometer simply were not obeyed by the mechanics.

When the electron diffraction patterns are collected every 1°, many high-resolution reflections with d-spacings smaller than 1 Å are completely missing. Even at 0.2° steps, the sampling can be too sparse, so that the high-resolution reflections (outside 1 Å resolution) are only recorded on a single frame. Similar behavior can be found in the electron beam rotation which is discussed below. The beam tilt step is considered to be optimal if the highest resolution reflections (in the range 0. 7Å–0.5 Å) can be recorded on at least 4–5 consecutive frames. To achieve these numbers, the beam tilt step should be as small as 0.05°. If the beam rotation range is more than 2°, the alignment of the electron beam rotation becomes critical, and also the distortion of the electron beam can appear forming an ellipse-shaped disk in the NBD mode. Thus, in our data collection procedures we used the limits for the beam tilt as ±2°.

In the second experiment, after 80 steps of 0.05° consecutive electron beam rotations (adding up to 4° total beam tilt) the goniometer was rotated by 3.5° creating a 0.5° overlap between two rotation series. In our case the TEM goniometer allowed ±40° tilts which produced 23 sets of 80 frames each. Altogether ∼1800 frames were recorded. Then similar SAED patterns were found in the overlapping areas of neighboring data sets (Figs. 2b, 2c). In this case the magnitude of the goniometer rotation angles could be accurately calibrated. For example, in that case, the crystal was actually rotated by 3.7° instead of the 3.5° requested by the program.

In order to demonstrate the rotation of the electron beam, a series of electron diffraction patterns close to the [001] zone axis were selected as shown in Fig. 3. When the electron beam is rotated by a step of 0.05°, the differences between neighboring patterns are very small. However, changes between the first (0°) and the last frames (0.35°) are dramatic. The position of the direct beam on the CCD camera remains at exactly the same position in all these patterns (within ∼1 pixel) which simplifies the further data processing.

As the rotation angle changes, new reflections become strong coming close to the exact Bragg condition. Finally, diffraction patterns were summed up, combining 80 frames which represent a tilt range of 4°. The final patterns close to and far away from the zone axis are shown in Figs. 4a and 4b, respectively. There were only $hk0$ reflections in the dataset collected close to the [001] zone axis. The final frame representing the sum of diffraction patterns in the data set recorded far away from that zone axis contains narrow bands of reflections. Each band has unique l Miller index representing the corresponding reciprocal layer.

It should be noticed that the summed frames are clear and do not have any spot splitting or elongations. This proves that the positions of the same reflection on consecutive electron diffraction patterns within the series do not change. The combined patterns were analyzed using the ELD program (supplementary Fig. S2). There were only some minute positional distortions for the ultra high angle reflections which could easily be corrected by data processing. In Fig. 4a, the reflections near the rotation axis are stronger than the others. This is due to the fact that these reflections are close to the Bragg condition on many exposure frames, *i.e.* they have much finer sampling.

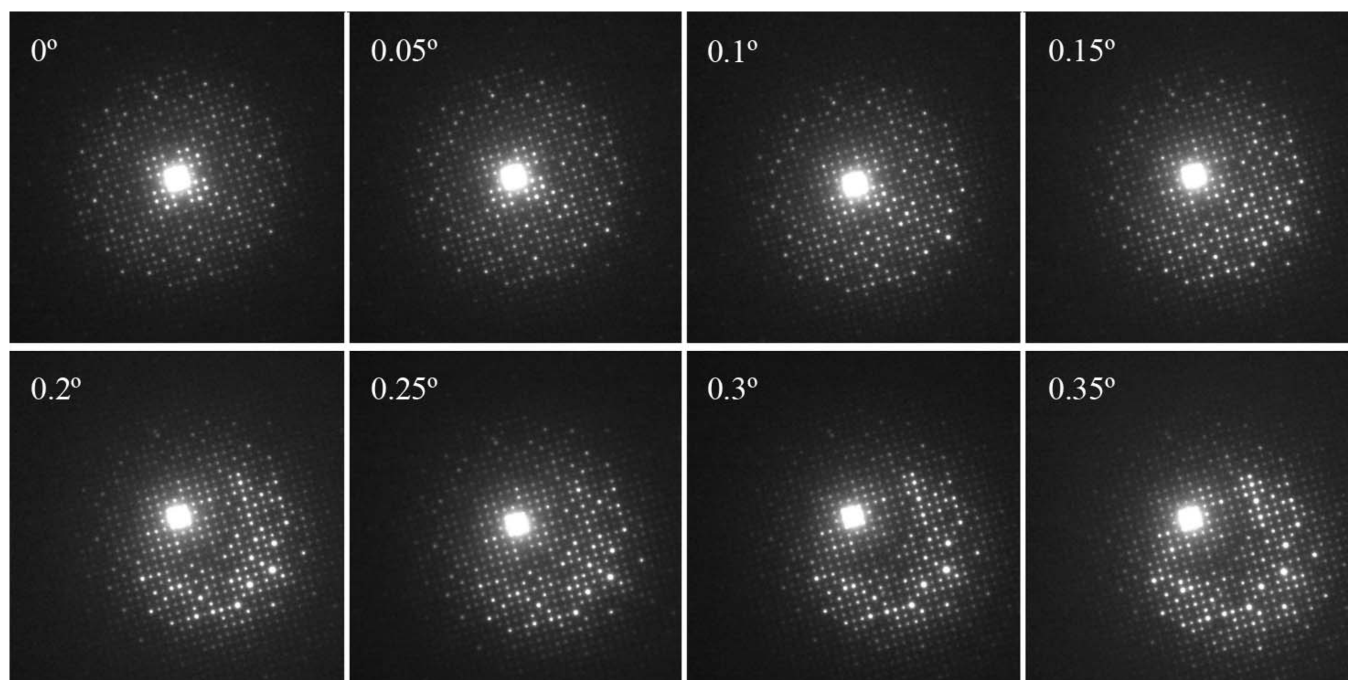

Fig. 3. High precision beam tilt series of 0.05° interval performed by the rotation method. The electron beam was tilted slowly away from the [001] zone axis at 0°, while the direct beam was kept at the same position.

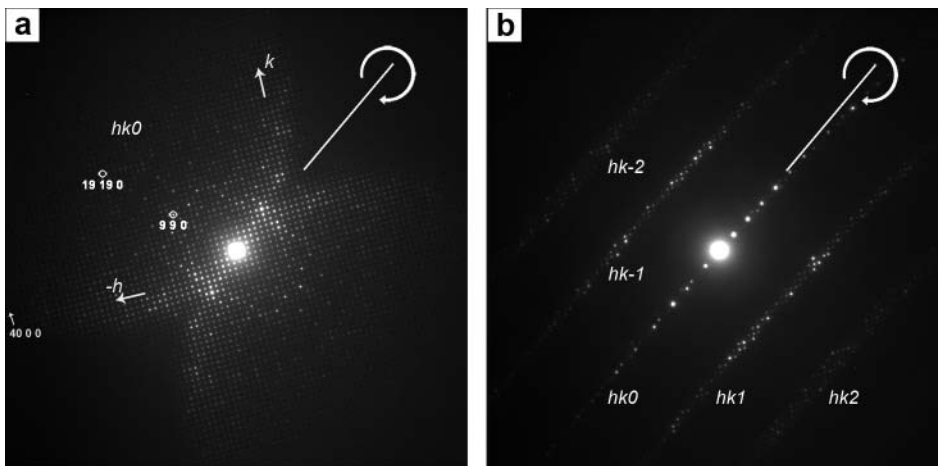

Fig. 4. 80 frames of 0.05° rotation step are summed into combined diffraction patterns of 4° rotation. The rotation axis is marked by lines. (**a**) is very close to the [001] zone axis and contains most of the reflections in the *hk*0 layer. The furthest reflections are at a resolution of 0.46 Å (Note the 4 mm symmetry, which can be seen up to more than 40 diffraction orders. The reflections (9 9 0) and (19 19 0) mentioned in the text are marked. (**b**) is another beam tilt set; −22° to −18°. The central narrow line contains *hk*0 reflections; the broader bands contain *hk*1 and *hk*2 (below) and *hk* −1 and *hk* −2 reflections (above).

3.1 Corrections for geometrical (Lorentz) factors

The geometrical or so-called Lorentz factor is proportional to the time the reflection spends close to the exact Bragg condition and inversely proportional to the velocity with which the Ewald sphere passes through the diffraction condition. The influence of the Lorentz factor on different reflections can be demonstrated as follows. The (9 9 0) reflection ($d_{(990)} = 2.16$ Å) and the (19 19 0) reflection ($d_{(19\ 19\ 0)} = 1.02$ Å) marked in Fig. 4a are located on the line perpendicular to the rotation axis. The (19 19 0) is at a distance of 1.0 $Å^{-1}$ away from the rotation axis. This is approximately twice as far as (990) which is at 0.5 $Å^{-1}$. Thus the Ewald sphere will sweep through (19 19 0) twice faster, so that there will be only half as many sampling points for the (19 19 0) as compared to the (9 9 0), *i.e* it will be seen on half as many frames in the series. At the same time, the excitation errors can be calculated using geometric relations. The strongest intensities will appear at the exact Bragg condition. The curves representing profiles of the (9 9 0) and (19 19 0) reflections are given in Fig. 5. Intensities of certain reflections from different electron diffraction patterns were plotted as a function of the excitation error. Basically, integrated intensities should be equal to the area under the curve when the reflection profile is plotted against the excitation error. Then different samplings for low and high angle reflections will not affect the integrated intensity values. The number of sampling points (*i.e.* frames) should be ≥ 4 within the double full width half maximum (FWHM) to describe the shape of the peaks. In this way, the Lorentz factor which is considered in single crystal X-ray diffraction is taken care of.

3.2 Sampling

It becomes obvious analyzing the intensity curves (see Fig. 5) that at least 0.20° and 0.10° beam rotation steps are needed to make fine enough sampling of the (9 9 0) and (19 19 0) reflections, respectively. Otherwise, the shape of the reflection curve is poorly defined because of the sparse sampling. Often sub-Ångström diffraction data is required for accurate crystallographic studies. Therefore, electron beam rotation with very fine step ($\leq 0.10°$) is necessary for high resolution 3D reconstruction of reciprocal space. In our case, the half-widths of the reflections were so small that 0.05° rotation steps resulted in only 3 sampling points for the outermost reflections. These reflections have *d*-values of 0.6 Å. If only data to lower resolution is to be collected, for example limited to 1 Å or even 2 Å resolution, the step size can be increased to 0.10° and 0.20°, respectively.

3.3 Data processing

The data from all series will finally be combined into a 3D data set for reciprocal space reconstruction, representing a part of reciprocal space that has been sampled. This work will be done by a post data processing program which we are currently working on. After reciprocal space is reconstructed, all the reflections can be indexed. For a crystal with unknown structure, the unit cell dimensions and space group can also be determined. When the integrated intensities of all the reflections are estimated, *hkl* files can be produced and used for solving the structure.

3.4 Data collection strategies

Another issue is the complete coverage of reciprocal space. In our case, having a crystal with the tetragonal symmetry *P*4/*mbm*, a general *hk*0 reflection appears 8 times while a general *hkl* reflection appears 16 times (8 times as *hkl* and another 8 times as *hk* −*l*). In other words, we only need to reconstruct $^1/_{16}$ of reciprocal space to get a complete 3D reflection data set. For structures with lower symmetries, more coverage of reciprocal space during data collection is needed. In the X-ray rotation method the beam is fixed, while the crystal is rotated around an axis perpendicular to the beam. The crystal can easily be rotated a full 360°. All 3D diffraction data can be collected, except a so-called "missing cone" along the crystal rotation axis. The missing data may be collected from the same or another crystal, mounted in a different orientation. The sample holder available to us for the present work only allows 80° (±40 °) goniometer tilt. High tilt tomography holders are helpful for collecting even more complete data on a single crystal. Another alternative is to combine partial diffraction data sets from different crystals. Once all the reflections are indexed and inten-

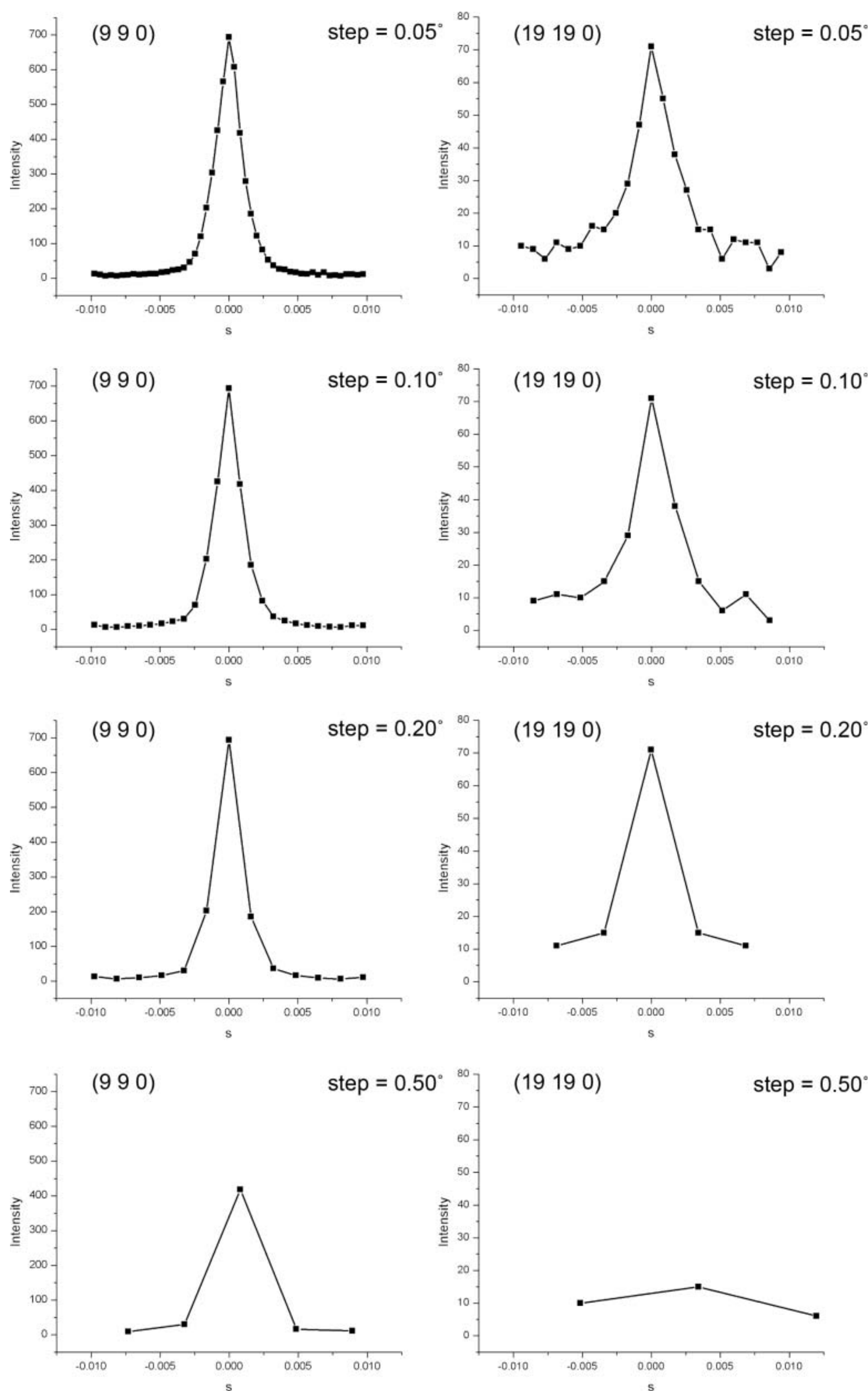

Fig. 5. Intensity curves of the (9 9 0) and (19 19 0) reflections are shown at 0.05°, 0.10°, 0.20° and 0.50° tilt intervals with diffractive intensities and excitation error as the vertical and horizontal axes. The unit of the horizontal axes is $Å^{-1}$. While a step size of 0.20° is sufficient for a reflection of intermediate resolution, such as the (9 9 0) (*d*-value 2.16 Å), the steps must be $\leq$0.10° for high resolution reflections, such as (19 19 0) (with *d*-value 1.02 Å). Note that the horizontal scale is the same for all eight diagrams, while the vertical axes of the left and right columns are in different absolute scales.

sities have been integrated, data from different crystals can be merged, using the common reflections for scaling. This can be done by standard crystallographic programs such as SHELX (Sheldrick, 2008) or Triple (Calidris).

4. Conclusions

While precession electron diffraction is superb for obtaining high-quality near-kinematical data for individual zone axes,

rotation data is better suited for collecting complete 3D electron diffraction data. We have presented a new data collection method combining goniometer rotation and beam rotation with very fine steps. Not only the data collection but also the alignment and calibration procedures are all automatic, which opens new applications for those crystallographers and material scientist who are not experts in TEM operations. By this rotation method, reciprocal space can be reconstructed with very high resolution. Thus, it also gives new possibilities to answer physical and electron crystallographic questions, such as the effect of dynamical and secondary scattering. Electron crystallography can then be a worthy complement to X-ray crystallography, but applicable to crystals a million times smaller than the smallest envisioned even for synchrotrons. If measures are taken to minimize the electron beam damage, this technique may also be applied to organic molecules and even to proteins, allowing full 3D electron diffraction data sets from crystals of unprecedented small sizes to be collected.

Acknowledgments. The Swedish Science Research Council (Vetenskapsrådet) and Göran Gustafsson Foundation are thanked for financial support. The electron microscopes used were purchased from a grant given by the Knut and Alice Wallenberg Foundation.

References

Arndt, U.W.; Wonnacott, A.J. (Eds.): The Rotation Method in Crystallography. North Holland, Amsterdam, (1977).

Avilov, A.; Kuligin, K.; Nicolopoulos, S.; Nickolskiy, M.; Boulahya, K.; Portillo, J.; Lepeshov, G.; Sobolev, B.; Collette, J.P.; Martin, N.; Robins, A.C.; Fischione P.: Precession technique and electron diffractometry as new tools for crystal structure analysis and chemical bonding determination. Ultramicroscopy **107** (2007) 431–444.

Baerlocher, C.; Gramm, F.; Massüger,L.; McCusker, L.B.; He, Z.B.; Hovmöller,S.; Zou, X.D.: Structure of the Polycrystalline Zeolite Catalyst IM-5 Solved by Enhanced Charge Flipping. Science **315** (2007) 1113–1116.

Bhide, V.; Gasparin, M.: A new GTB-type thallium niobate. Acta Cryst. B **35** (1979) 1318–1321.

Capitani, G.C.; Oleynikov, P.; Hovmöller, S.; Mellini, M.: A practical method to detect and correct for lens distortion in the TEM. Ultramicroscopy **106** (2006) 66–74.

Cowley, J.: Electron Diffraction Techniques, Vol. 1, IUCr, Oxford University Press, 1992.

Dorset, D.L.: Structural Electron Crystallography, Plenum Press: New York (1995).

Gemmi, M.: Electron Crystalloggraphy and cryoelectron microscopy on inorganic materials and organic and biological molecules. Precession electron diffraction in EUROSUMMER SCHOOL, Barcelona (Spain), (2001).

Gjønnes, J.; Hansen, V.; Berg, B.S.; Runde, P.; Cheng, Y.F.; Gilmore, C.J.; Dorset, D.L.: Structure model for the phase AlmFe derived from three-dimensional electron diffraction intensity data collected by a precession technique. Comparison with convergent beam diffraction. Acta Crystallogr A **54** (1998) 306–319.

Gramm F.; Baerlocher, Ch.; McCusker, L.B.; Warrender, S.; Wright P.A.; Han, B.; Hong S.B.; Liu, Z.; Ohsuna T.; Terasaki, O.: Complex zeolite structure solved by combining powder diffraction and electron microscopy. Nature **444** (2006) 79–81.

Henderson, R.; Unwin, P.N.T: Three-dimensional model of purple membrane obtained by electron microscopy. Nature **257** (1975) 28–32.

Kolb, U.; Gorelik, T.; Kübel,C; Otten,M.T.; Hubert,D.: Towards automated diffraction tomography: Part I—Data acquisition, Ultramicroscopy **107** (2007) 507–513.

Moukhametzianov, R.; Burghammer, M.; Edwards, P. C.; Petitdemange, S.; Popov, D.; Fransen, M.; McMullan, G.; Schertlera, G. F. X.; Riekel, C.: Protein crystallography with a micrometre-sized synchrotron-radiation beam. Acta Crystallogr. D **64** (2008) 158–166.

NanoMEGAS, http://www.nanomegas.com/

Own, C.S.; Subramanian, A.K.; Marks, L.D.: Quantitative Analyses of Precession Diffraction Data for a Large Cell Oxide. Microscopy and Microanalysis **10** (2004) 96–104.

Sheldrick, G.M.: A short history of SHELX. Acta Cryst. A **64** (2008) 112–122.

Vainshtein B. K.: Structure analysis by electron diffraction. Pergamon Press (1964).

Vincent, R.; Midgley, P.A.: Double conical beam-rocking system for measurement of integrated electron-diffraction intensities. Ultramicroscopy **53** (1994) 271–282.

Weirich, T.; Ramlau, R.; Simon, A.; Zou, X.D.; Hovmöller, S.; A crystal structure determined to 0.02 Å accuracy by electron microscopy. Nature **382** (1996) 144–146.

Weirich, T.E.; Zou, X.D.; Ramlau, R.; Simon, A.; Cascarano, G.L.; Giacovazzo,C,; Hovmöller,S.: Structures of nanometre-size crystals determined from selected-area electron diffraction data. Acta Cryst. A **56** (2000) 29–35.

Zou, X.D.; Mo, Z.M.; Hovmöller, S.; Li, X.Z.; Kuo, K.: Three dimensional reconstruction of the ν-AlCrFe phase by electron crystallography. Acta Cryst. A **59** (2003) 526–539.

Zou, X.D.; Sukharev, Y.; Hovmöller, S.: ELD – A Computer Program System for Extracting Intensities From Electron Diffraction Patterns. Ultramicroscopy **49** (1993) 147–158.

Zvyagin, B. B.; Zhukhlistov A. P.; Nickolsky M. S.: Minerals – a special area of electron diffraction structure analysis. Z. Kristallogr. **218** (2003) 316–319.

Collecting 3D electron diffraction data by the rotation method

Daliang Zhang, Peter Oleynikov, Sven Hovmöller* and Xiaodong Zou

Structural chemistry, Stockholm University, SE-106 91 Stockholm, Sweden

Received

Keywords: Electron diffraction, data collection, 3D diffraction data

Abstract

A new method for collecting complete three-dimensional electron diffraction data is described. Diffraction data is collected by combining electron beam tilt at many very small steps, with rotation of the crystal in a few but large steps. A number of practical considerations are discussed, as well as advantages and disadvantages compared to other methods of collecting electron diffraction data.

Contents

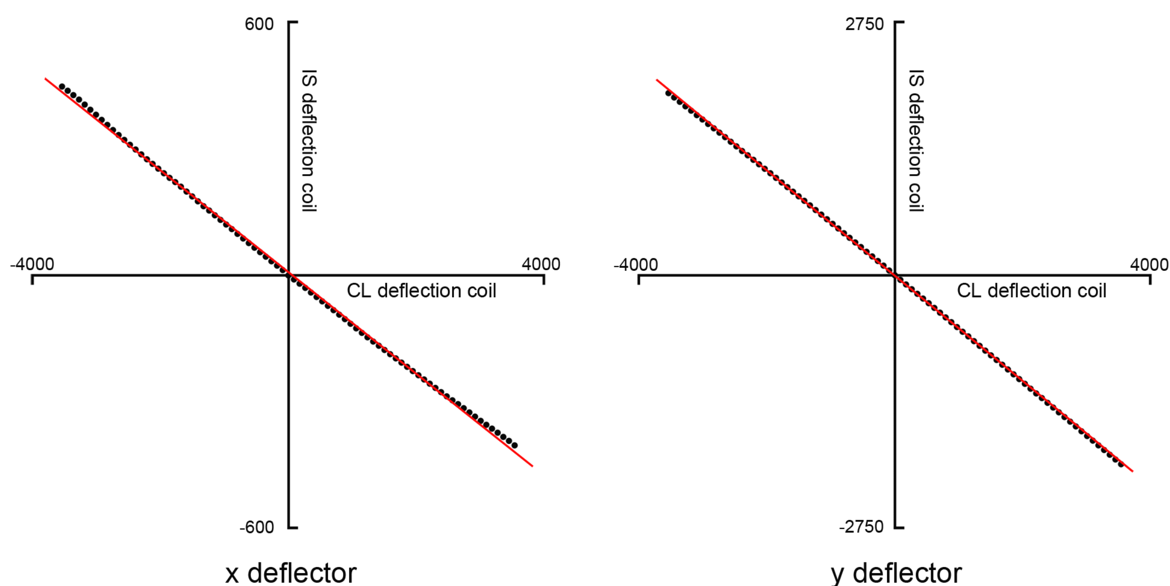

Figure S1.The ratio between the beam tilt and corresponding x- and y- image shift (IS) deflection coil values must be calculated. This ratio can be calculated from 81 points for different condenser lens (CL) deflection coil tilts in the range from –2˚ to 2˚ (0.05˚ step). Each plot represents the variation of IS deflection coil values (shifts) against the CL deflection coil values (tilts). Both plots show linear behavior for x- and y- deflectors. The unit of the horizontal and the vertical axes are given in JEM 2100 TEM corresponding coil digital units.

* Corresponding author: Sven Hovmöller, svenh@struc.su.se

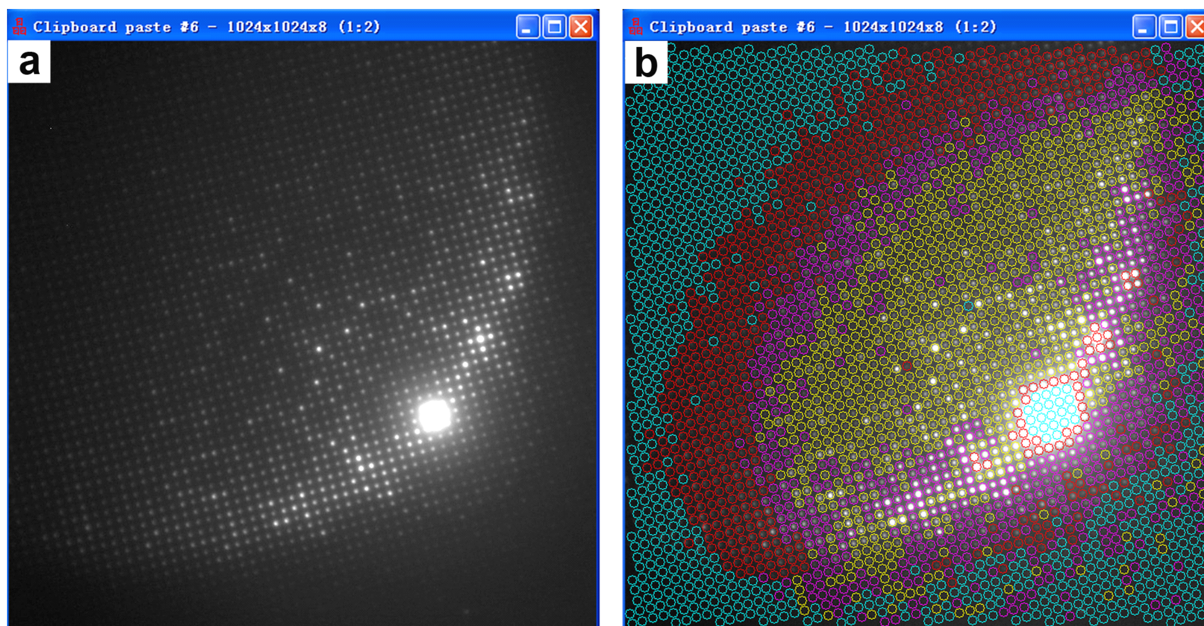

Figure S2. a) is a combined diffraction pattern of 2º rotation close to the [001] zone axis. The reflections are hk0 reflections. b) is a screen-shot from ELD showing that high-resolution reflections do not fall exatly on the same lattice as the low-resolution reflections do. The reflections marked by yellow, pink, red and blue rings represent ‘good intensity and position’, ‘good intensity but misplaced’, ‘impossible to estimate’ and ‘too weak’ reflections.